Mechanical Systems and Signal Processing 244 (2026) 113803

Contents lists available at ScienceDirect

Mechanical Systems and Signal Processing

journal homepage: www.elsevier.com/locate/ymssp

Full Length Article

Multi-sensor estimation algorithm for the friction coefficient and the braking torque of carbon braking systems for racing motorcycles

Federico Bonini, Alessandro Rivola, Marco Troncossi, Alberto Martini *

DIN – Dept. of Industrial Engineering, Alma Mater Studiorum - University of Bologna, Italy

ARTICLE INFO

Communicated by Pietro Borghesani

Keywords:
Machine learning
Carbon brakes
Artificial neural network
Friction coefficient
Nonlinear autoregressive exogenous model

ABSTRACT

This paper investigates new methods for estimating the braking torque generated by carbon brakes mounted on MotoGP^{TM} class motorcycles. A physical model of the brake was originally implemented in order to calculate the torque applied to the motorcycle front wheel using the measured brake fluid pressure and the braking system geometry as inputs. The results obtained with this method are currently limited by the usage of a constant friction coefficient in the equations of the model. Since it is extremely hard to estimate the friction coefficient using a classical model-based approach, it was deemed more convenient to develop a machine learning algorithm capable of identifying the friction coefficient in any operating condition of the brake. To this purpose, different machine learning models were evaluated and compared, paying particular attention to the dataset generation and to how the labels used as targets during training were calculated. An algorithm combining a Nonlinear Autoregressive Exogenous model (NARX) and an Artificial Neural Network (ANN) was finally selected and trained. The developed algorithm was successfully tested on several datasets collected during experimental tests on different tracks, providing satisfactory results in terms of braking torque estimation and friction coefficient identification.

1. Introduction

In the past few decades brakes made of carbon composites have become the dominant technology for high-performance braking systems [1,2]. Indeed, they are a convenient solution in applications where light weight and high friction coefficient at high temperature represent essential specifications, such as brake assemblies of aircraft landing gears [3,4] and sports/racing cars/motorcycles [5,6].

This research activity is promoted by a motorcycle manufacturer, namely the company Ducati Corse (a division of Ducati Motor Holding S.p.A., Bologna, Italy) and focuses on the estimation of the braking torque provided by the carbon brakes adopted for the motorcycles competing in the MotoGP^{TM} world championship. Indeed, the racing performance is heavily affected by the vehicle behavior during braking maneuvers. Hence, assessing reliably the available braking torque is essential in order to arrange alternative configurations and/or draw up new strategies to possibly improve race results.

The studied braking system features discs made up of carbon–carbon composite, i.e. having both the matrix and the reinforcing

* Corresponding author.
E-mail address: alberto.martini6@unibo.it (A. Martini).

https://doi.org/10.1016/j.ymssp.2025.113803
Received 24 October 2025; Accepted 21 December 2025
Available online 29 December 2025

Nomenclature

Acronyms and abbreviations

ANN	Artificial neural network
DT	Decision tree
E#	#-th method for friction coefficient estimation
FE	Finite Element
LightGBM	Light Gradient-Boosting Machine
MCCP	Minimal Cost-Complexity Pruning
ML	Machine learnig
MLP	Multilayer perceptron
NARX	Nonlinear autoregressive exogenous model
NDA	Non disclosure agreement
SVM	Support vector machine
TR-&#	#-th dataset related to the generic racetrack "&"
UKF	Unscented Kalman Filter
1D	One-dimensional

Symbols

A_p	Brake piston total cross section [m^2]
b	NARX bias array
E_{diss}	Dissipated Energy [J]
F_n	Carbon pads total normal force (magnitude) [N]
$\mathbf{F}_t$	Brake disc tangential force [N]
IW	NARX weight matrices
K_μ	Braking torque amplifyng factor
LW	NARX weight matrices
P_c	Corrected brake fluid pressure [Pa]
P_m	Brake fluid pressure [Pa]
P_{NARX}	NARX estimate of the pressure signal P_s [Pa]
P_s	Modified pressure signal [Pa]
P_{th}	Pressure threshold [Pa]
R_{eff}	Effective radial distance at which F_t is applied [m]
T_{acp}	Average disc/pads contact patch temperature calculated using the thermal model of the brake [K]
T_d	Carbon disc lateral surface temperature measured by the single spot transducer [K]
T_i	Initial disc temperature [K]
T_{track}	Track temperature [K]
t	Braking time: sawtooth signal that keeps track of the time elapsed from the beginning of each braking maneuver
t_e	Braking maneuver duration
t_1	Instant at which the braking maneuver begins [s]
t_2	Instant at which the friction coefficient computed by the inverted feed-forward model comes back within a prescribed percentage of the reference value [s]
n_y	Number of previous values of the NARX output signal
n_u	Number of previous values of the NARX independent input signal

Greek symbols

ΔT	Single spot and 1D-FE model temperature difference [K]
ε_p	Arbitrary threshold used for calculating the P_c signal
μ	Brake friction coefficient
μ_{const}	Nominal (constant) brake friction coefficient
τ_{bf}	Braking torque generated on the front wheel [Nm]
ω_r	Disc/pads relative angular velocity [rad/s]

fibers made up of carbon, hence being frequently referred to as C/C brakes. At present, the company estimates the amount of braking torque provided by the front braking system by using an analytical model that has the instantaneous brake fluid pressure (measured on board) as input (see Section 2). After each test session (with one or more consecutive laps) the telemetry data are downloaded from the motorcycle (real-time telemetry is forbidden by the championship rules) and processed with various algorithms, including the one for braking torque estimation, in order to evaluate possible modifications of the vehicle setup for enhancing its performance. However, the effectiveness of the current model is reduced by the limited knowledge of the instantaneous friction coefficient between disc and pads. Indeed, the friction coefficient of carbon–carbon brakes is known to be largely affected by at least three state variables characterizing

the system operating condition (namely, disc temperature, relative speed between disc and pads, and brake fluid pressure), with a highly nonlinear relation [5,7–9]. Only limited information on the friction coefficient mapping is available from the brake manufacturer. In addition, carrying out experiments on a test rig to cover the wide range of operating conditions possibly experienced during races appears unfeasible: besides being too costly and time consuming, it would be extremely hard to cope with the fast evolution of the system of interest, with new variants and configurations being continuously developed. Finally, in light of the above mentioned nonlinear dependence on many factors, modelling analytically the trend of the friction coefficient seems impractical [10].

This issue can be partially solved by assuming reasonable values of the friction coefficient obtained from the literature, or by imposing an average friction coefficient derived from experimental measurements performed during specific tests [3,4]. However, the use of a constant friction coefficient still results in significant discrepancies between the data measured experimentally and the values predicted by the model.

Only few studies on the identification of the friction coefficient of brakes can be found in the literature, all the works dealing with passenger cars, i.e. vehicles equipped with steel/iron brake discs and undergoing moderate dynamic transients with respect to racing vehicles [11]. An analytical model of the friction coefficient that takes into account the brake dynamics has been proposed in [12]. However, some inaccuracies in case of fast transients have been identified [11]. The use of a linear Kalman Filter for the identification of the braking torque, that can be used to estimate the friction coefficient, has been investigated in [10,11]. Since the identification relies on a good estimation of the tire forces, it is not deemed completely viable for the case of interest. Indeed, the tire slip can reach large values in racing motorcycles, hence its estimation being also challenging, and possibly affected by uncertainty and noise. Machine Learning (ML) algorithms proved quite effective in predicting the braking performance [13]. In [14] the use of an Artificial Neural Network (ANN) to estimate the braking torque from three input operating conditions (namely, brake fluid pressure, initial disc interface temperature and disc speed at the beginning of the braking maneuver) has been investigated. The same 3 quantities and 23 additional parameters related to material composition and manufacturing process of the brake pads have been used as inputs to identify the brake factor (i.e., twice the friction coefficient) with different ANN architectures trained with different algorithms in [15,16]. In [17] ANNs have been adopted to predict how the friction coefficient is affected by the amount of two materials included in the composition of the brake pads. In [18], the friction coefficient has been estimated with a multilayer perceptron (MLP) ANN by choosing the sliding speed, sliding acceleration and contact pressure as input parameters. In [19] a non-linear autoregressive network with exogenous inputs (NARX) has been used for predicting the braking torque from brake fluid pressure, and initial temperature and speed of the disc. In [20] an Elman ANN has been adopted to identify the friction coefficient from initial disc speed and temperature, brake fluid pressure, loading history of the brake, and 16 further inputs related to the material composition of the pads. All the works using ML algorithms dealt with experiments conducted on test rigs with laboratory grade sensors. To the authors' best knowledge, no works concerning friction coefficient identification in carbon–carbon brakes and/or in racing applications in real-world operation are available. Apparently, robust and effective tools for assessing the instantaneous braking torque of such systems are not available either.

This work aims at developing an algorithm for braking torque estimation of high-performance brakes in actual operating conditions, through the implementation of ML-based algorithms to identify the instantaneous friction coefficient characterizing the system. The final goal is achieving a more accurate braking torque estimation to possibly satisfy also the stringent requirements of the MotoGP^{TM} competition in terms of reliability and performance. The ML approach (in particular, supervised algorithms) is deemed particularly convenient for the application of interest, due to the possibility of collecting a very large amount of data (measured by multiple sensors on the motorcycle) from both track tests and racing sessions (also with different motorcycle configurations and/or riders), to be adopted for training and verifying the implemented algorithm [21]. The desired algorithm should process the signals normally available during a race from the motorcycle telemetry and from other measurements performed in the racetrack (e.g. air and tarmac temperature). Even though the algorithm is not required to run in real-time, it must provide the best trade-off between accuracy and computational complexity in order to be able to process the large amount of data collected in several full laps during each test session before a race. Indicatively, it is expected to take less than 10 s per lap to possibly allow the racing team to modify the motorcycle set up between two test sessions. Moreover, the algorithm may be used also in a different scenario, for processing data generated by (lap-time) simulations of entire races. In this case, while more time may be available for performing the analyses, computational efficiency is still deemed essential, due to the increased amount of data to be handled.

The main focus is on the implementation of an ANN-based algorithm [22], in light of the promising results achieved in the works mentioned above. Many different architectures of the network have been implemented and tested with MATLAB (Mathworks, Natick, MA, USA), by using as inputs the measured instantaneous values of the disc temperature, the brake fluid pressure and the wheel speed, belonging to a restricted dataset. A NARX has been also developed to improve the reliability of the pressure signal before entering the ANN. The possibility of improving the algorithm accuracy by expanding the input vector with additional signals has been also successfully assessed. Then, the performance of the ANN-based algorithm has been compared with other ML approaches that were deemed potentially suitable for friction coefficient estimation, namely Support Vector Machines (SVM) [23] and Decision Trees (DT) [24] through the MATLAB Regression Learner package, and Light Gradient-Boosting Machine (LightGBM) [25]. Finally, the resulting algorithm, which combines the NARX and the optimized ANN, has been trained with an extended dataset, and then tested on several additional datasets collected through measurements conducted by running various laps in different racetracks, for a comprehensive evaluation of its performance. This allowed to map the friction coefficient over a wide range of operating conditions.

The paper is structured as follows. The mechanical model of the braking system under investigation is presented in Section 2. In Section 3, the data available for the study and the signal processing methods are discussed. All the phases of the ML algorithm development and testing are described in Section 4. The main results provided by the implemented version of the algorithm are reported in Section 5. Finally, the conclusions are drawn in Section 6.

2. Braking system analytical model

A schematic of the carbon braking system installed in the front wheel of MotoGP™ class motorcycles is shown in Fig. 1. The floating carbon disc (or rotor) is connected to the wheel rim (not shown in the image) by the rotor carrier, whereas the caliper is connected to the front fork tube by a rigid support (not shown in the image). The two carbon pads are pushed against the disc by two pistons each, with a total normal force of magnitude F_n, given by

$$F_n = A_p \bullet P_m \tag{1}$$

where A_p is the total cross section of the four pistons and P_m is the pressure of the brake fluid. This generates a tangential friction force acting on the disc, $\mathbf{F}_t$, that opposes to the disc/pads relative angular velocity, $\boldsymbol{\omega}_r$. The front wheel is equipped with two discs (one on each side of the rim, with its own caliper). The magnitude of the braking torque generated on the front wheel, τ_{bf}^{mod}, can be determined by using the following expression:

$$\tau_{bf}^{mod} = 2\mu \bullet F_n \bullet R_{eff} \bullet K_\mu \tag{2}$$

where μ is the friction coefficient; R_{eff} is the effective radial distance at which $\mathbf{F}_t$ is applied; the parameter K_μ is an amplifying factor, which is a rational function of μ related to the specific caliper geometry (its exact expression cannot be provided due to non-disclosure agreements – NDA); the factor 2 is related to the presence of two brake discs (with two distinct calipers) on the front wheel.

The model is currently exploited by the motorcycle manufacturer by assuming a constant value, μ_{const}, for the friction coefficient. Such value has been defined on the basis of the company database and experience to fit a large portion of the breaking maneuvers performed in the racetracks of the MotoGP™ championship. However, large variations of the instantaneous μ may be experienced when the operating conditions of the brake (primarily the disc temperature, the brake fluid pressure and the disc/pads relative angular speed) differ remarkably from the most common values, leading to significant discrepancies between the real and the predicted braking torque. Therefore, the research is aimed at achieving a more accurate calculation of the braking torque on the front wheel by estimating the instantaneous μ through a ML algorithm.

It's worth noting that, instead of predicting the friction coefficient, ML tools could be trained to directly estimate the value of the braking torque, without the need to build the physical model outlined by Eq. (2). However, calculating the braking torque through the analytical model is deemed more convenient since it permits to assess the effects of different design parameters of the braking system without the need of retraining the algorithm. In fact, MotoGP™ teams are allowed to choose different brake discs and pads according to the characteristics of each track. This approach allows to take into account these multiple solutions simply by changing the parameters of the physical model (in particular the effective radius and the amplification coefficient K_μ) instead of retraining the algorithm for every possible combination of braking system design parameters.

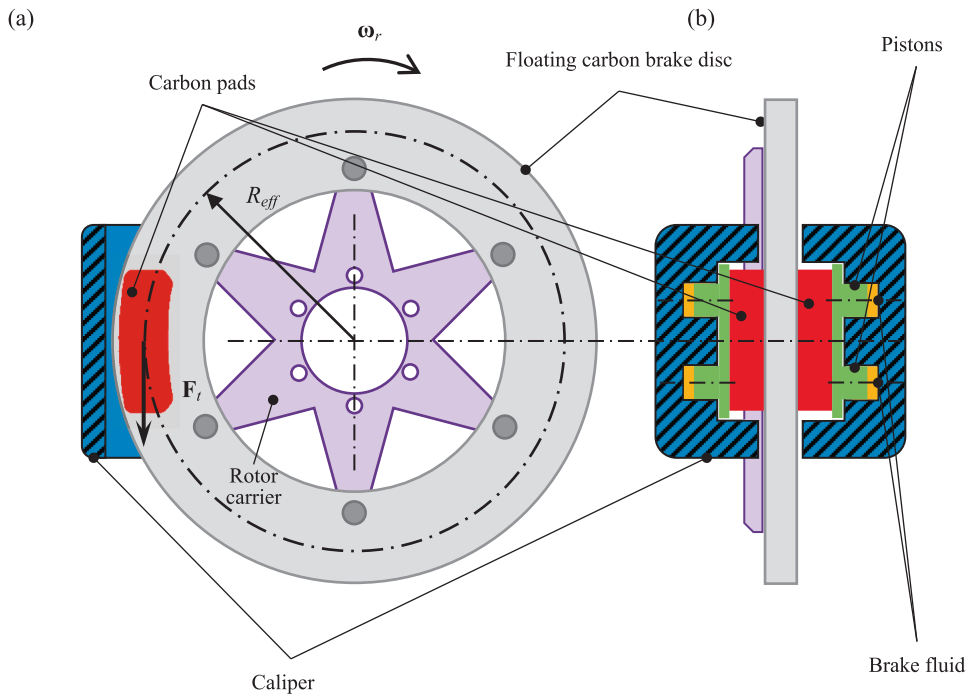

Fig. 1. Schematic of the braking system: (a) side and (b) back view.

3. Experimental data acquisition and preparation

3.1. Available measurements

Numerous datasets have been collected by the motorcycle manufacturer in experimental tests performed on different racetracks and/or with different riders, and are available in the company database for this study. For each test session, a new set of discs and pads were installed, and several laps were run. Each dataset contains the signals measured by the transducers normally installed on board in the motorcycle racing configuration (all these sensors being handled by the acquisition system used for the motorcycle telemetry), including the following ones (for the sake of simplicity, only the quantities relevant for this study are reported):

- Temperature of the lateral surface of one carbon disc of the front wheel, referred to as T_d hereafter, measured by means of a single-point infra-red sensor at a fixed radial position in the disc/pad contact patch.
- Magnitude of the relative angular velocity of the wheel/disc with respect to the front fork/pads, referred to as ω_r, measured by using a non-contact speed sensor.
- Pressure of the brake fluid of the front wheel braking system, referred to as P_m hereafter, measured by a pressure transducer.

Data concerning the environmental conditions of the tests (e.g. temperature of the tarmac and wind speed) are also recorded in the datasets.

In addition, a special sensor setup (namely, a wheel torque transducer installed in the front assembly, not allowed during races) was arranged for directly measuring the magnitude of the braking torque on the front wheel, referred to as τ_{bf}^{exp} hereafter. The torque measurements were collected by means of the same acquisition system used for the motorcycle telemetry.

3.2. Dataset preprocessing

All the vehicle-related signals are synchronized (the acquisition system reads one channel at a time) and downsampled to a common sample rate of 100 Hz. Possible offsets and/or drifts of the torque sensor are removed by both applying detrending techniques and forcing the signal to exhibit a null mean value in the phase occurring before and after each breaking maneuver, i.e. when the brakes are not engaged (referred to as *brake-off* phase). Then, a new dataset (TR-&#) is generated for each test session by removing all the brake-off portions. Hence the resulting data consist of a sequence of braking maneuvers. A list of the datasets available for this study is reported in Table 1, with additional information on the disc temperature characterizing the corresponding test session, and on the dataset usage for the ML algorithm implementation. The following notation is adopted for the dataset name: the character "&" identifies a racetrack; the (increasing) number "#" indicates different versions of the dataset for a specific racetrack (i.e. updated with new data). About $2 \bullet 10^4$ samples are available for each quantity included in each dataset TR-&#. A portion of the dataset TR-A1, showing the trend of T_d, P_m and τ_{bf}^{exp} over six consecutive braking maneuvers is reported in Fig. 2 as an example. Due to NDA, the values are normalized with respect to a reference level for each quantity (for instance, the actual measured temperature, T_d, is divided by a reference temperature T_{ref}). The same operation is performed for the other quantities reported hereafter.

The actual friction coefficient characterizing the braking system during experimental tests, μ_{exp}, can be determined indirectly by substituting the measured quantities τ_{bf}^{exp} and P_m in Eqs. (1) and (2), obtaining

$$\mu_{exp} \bullet K_{\mu,exp} = \frac{\tau_{bf}^{exp}}{2F_n \bullet R_{eff}} \tag{3}$$

which can be solved analytically. The friction coefficient μ_{exp}, computed at each time step, is included in the datasets as an additional signal and is then used as the ground truth for training the ML algorithms, i.e. it represents the target value to be estimated.

Finally, additional experiments with a multi-spot temperature transducer (not reported in this work) have shown that the single-point onboard temperature measurement is not completely representative of the disc thermal behavior. Indeed, the disc can exhibit steep temperature gradients along its radius in hard braking. In order to achieve a better identification of μ with respect to temperature, it was deemed convenient to train the ML algorithms using the average temperature on the disc instead of the one measured by the single-spot sensor. Therefore, the measured signal T_d is further processed by using Bayesian filtering tools [26,27], in order to estimate the real temperature distribution on the disc, hence allowing ML algorithms to achieve a better identification of μ. In particular, a one-

Table 1
List of the datasets adopted.

Dataset	Disc temperature	Purpose
TR-A1	Average	Preliminary analysis and training
TR-A2	Average	Final training and optimization
TR-B	Average	Performance assessment
TR-H	High	Performance assessment
TR-L	Low	Performance assessment
TR-M	Average	Performance assessment

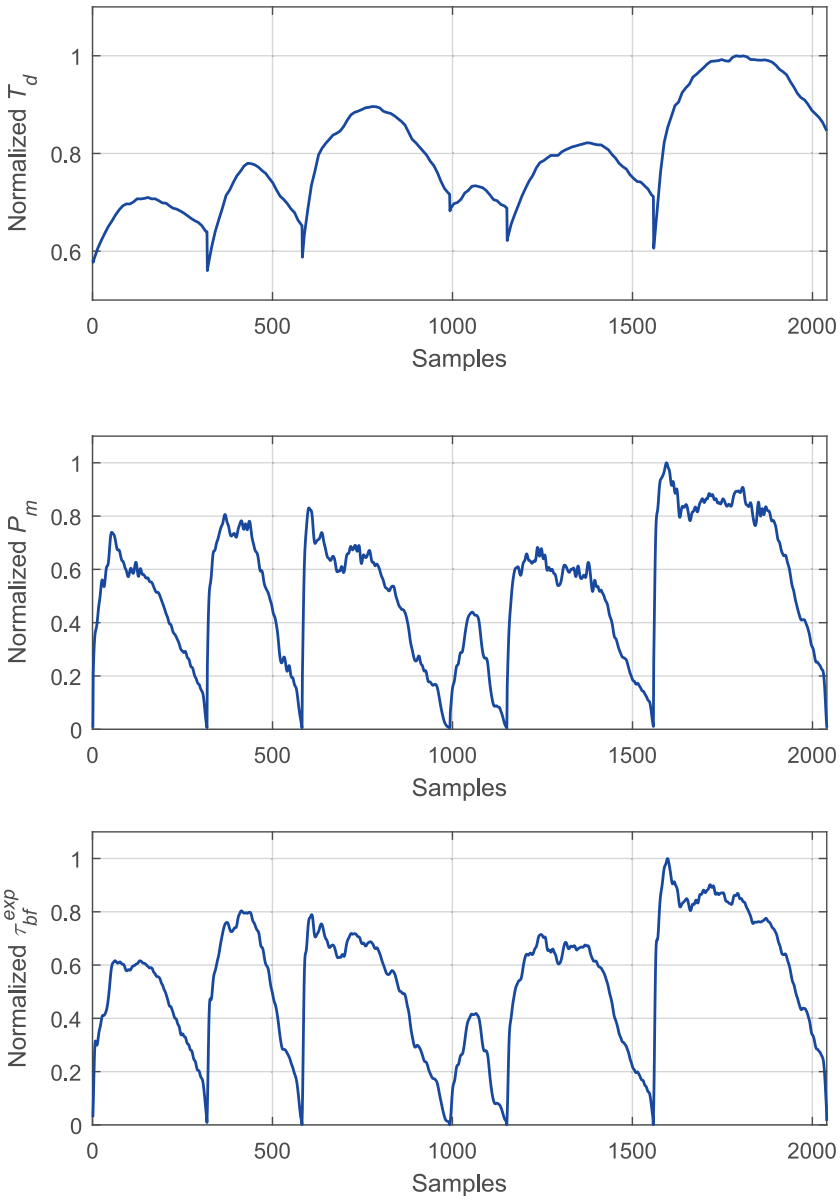

Fig. 2. Example of signals included in the database TR-A1.

dimensional Finite Element (1D-FE) thermal model of the disc is developed to predict numerically the temperature distribution as a function of the disc radius. Then, an Unscented Kalman Filter (UKF) is implemented and tuned to estimate the real temperature distribution on the disc surface, by combining the measured temperature T_d with the predictions of the FE model [28]. The UKF estimate is exploited to calculate an average temperature along the disc/pads contact patch, referred to T_{acp} that better represents the thermal state of the disc in the region of interest. The computed signal T_{acp} is fed into the subsequent ML algorithms (discussed in the following sections) in place of T_d. More in-depth information about the UKF and the 1D-FE model of the disc are provided in [29].

3.3. Dataset preliminary assessment

Fig. 3a reports the brake fluid pressure P_m and the breaking torque τ_{bf}^{exp} measured during three consecutive braking maneuvers (the first and the third maneuvers of the reported sequence are shown only partially). The trends of the signals measured by the two sensors appear not completely coherent. When the feed-forward model (properly inverted for the calculation of the friction coefficient) receives these signals, it outputs the unexpected positive and negative peaks in the friction coefficient trend (shown in Fig. 3b), which are deemed to lack any physical meaning. Such issue is experienced not only during the pressure build-up phase (particularly in the early

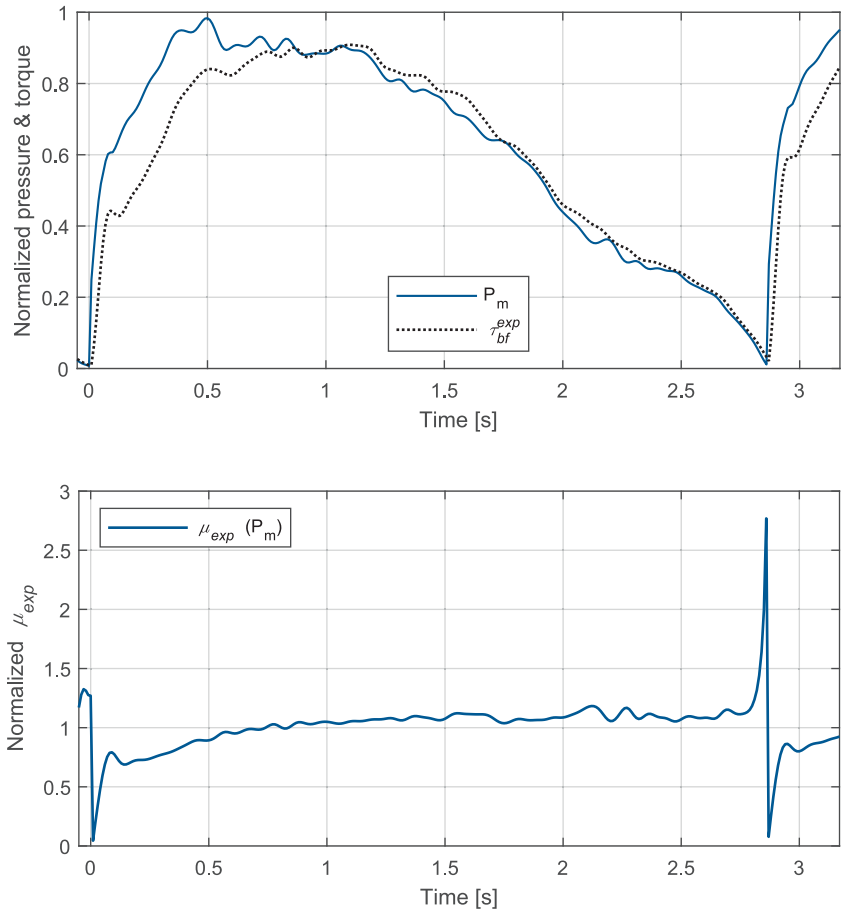

Fig. 3. (a) Normalized torque and pressure signals for the calculation of the true friction coefficient; (b) computed friction coefficient (normalized).

instants, characterized by the fastest transient), but also at the end of the breaking maneuver. The observed discrepancies may be partially related to the accuracy and hysteresis of the torque sensor that become more relevant for low values of the braking torque (being related to its full measuring scale), i.e. at the beginning and at the end of the braking maneuver. Moreover, pressure measurements were carried out by adopting the sensor setup of the race configuration, with the transducer installed close to the lever, hence possibly causing a different time response with respect to the torque transducer, that may be particularly relevant during the fast transient at the beginning of the braking maneuver. The friction coefficient computation depends on the ratio between the two signals, Eq. (3). This, in turns, may amplify the effects of measurement uncertainties when the numerator and the denominator become very small, hence possibly determining the peaks.

By disregarding the samples below a proper pressure threshold P_{th} (defined arbitrarily on the basis of the Company's knowhow) it is possible to remove the unrealistic behavior exhibited when the two signals are going back to zero. In practice, the friction coefficient is set at a value equal to μ_{const} whenever, at the end of a braking maneuver, the pressure falls below P_{th}. However, this procedure is not sufficient for the pressure build-up phase, due to the different dynamics. Indeed, at the beginning of the braking maneuver, the rider pulls the brake lever more aggressively, hence generating a sudden increment in both pressure and torque (pressure takes about 0.5 s to reach its maximum value, as shown in Fig. 3a). Conversely, when approaching to a corner (i.e. at the end of a breaking maneuver), the rider usually releases the brake very gently, hence resulting in slower transients (pressure takes about 2.4 s to go back to zero). Unlike in the latter phase, the discrepancies between the pressure and torque trends in the pressure build-up phase affects the signals throughout a wide pressure range (from zero to about 65 % of the pressure peak value, during about 0.2 s), and involve many samples above the pressure threshold previously set to deal with the ending phase of the maneuver. Therefore, further increasing the value of P_{th} is not a viable solution since too many samples would be neglected, hence causing the loss of essential information for training a ML algorithm.

Every braking maneuver exhibits a similar behavior in the early phase, but it is not repeatable enough to be correctly learned by a neural network. The disadvantage of using very complex networks is that they try to fit the data implementing extremely entangled relationships that dramatically reduce the training error but that completely fail to generalize to unseen samples due to the variability of this phenomenon. Therefore, when they are fed with values coming from another track or acquired in other conditions, their prediction is inaccurate.

3.3.1. Synthesized pressure signal

The strategy chosen in order to allow the analytical model to output more realistic values of the friction coefficient (for training the ML algorithms) is to estimate a pressure signal more consistent with the torque trend. To this purpose, a modified pressure signal (P_s) is generated for each braking maneuver. Such signal is synthesized by replacing the initial samples of the original (measured) pressure signal (P_m) with a fifth order polynomial, which better reflects the trend of the measured braking torque during the pressure build-up phase. In particular, a polynomial function of time in the form

$$g(t) = a_1 t^5 + a_2 t^4 + a_3 t^3 + a_4 t^2 + a_5 t + a_6 \tag{4}$$

is adopted. The vector of constant coefficients $\mathbf{a} = \{a_1, .., a_6\}$ is determined by imposing that the polynomial and its first and second derivatives are null at time t_1 and are equal, at time t_2, to the measured pressure $P_m(t_2)$, its first derivative $\dot{P}_m(t_2)$ and its second derivative $\ddot{P}_m(t_2)$, respectively, i.e. by solving the following linear system:

$$\begin{bmatrix} t_1^5 & t_1^4 & t_1^3 & t_1^2 & t_1 & 1 \\ 5t_1^4 & 4t_1^3 & 3t_1^2 & 2t_1 & 1 & 0 \\ 20t_1^3 & 12t_1^2 & 6t_1 & 2 & 0 & 0 \\ t_2^5 & t_2^4 & t_2^3 & t_2^2 & t_2 & 1 \\ 5t_2^4 & 4t_2^3 & 3t_2^2 & 2t_2 & 1 & 0 \\ 20t_2^3 & 12t_2^2 & 6t_2 & 2 & 0 & 0 \end{bmatrix} \begin{Bmatrix} a_1 \\ a_2 \\ a_3 \\ a_4 \\ a_5 \\ a_6 \end{Bmatrix} = \begin{Bmatrix} 0 \\ 0 \\ 0 \\ P_m(t_2) \\ \dot{P}_m(t_2) \\ \ddot{P}_m(t_2) \end{Bmatrix} \tag{5}$$

Time instant t_1 is when the braking maneuver begins (i.e., when the braking torque starts growing from zero). Time instant t_2 is when the friction coefficient computed by the inverted feed-forward model (Fig. 3b), after becoming almost null, comes back within a prescribed percentage of the reference value. Fig. 4 shows the comparison between the original (measured) signal, P_m, and the synthesized one, P_s.

Since the wheel torque transducer is not allowed during the race, the new pressure signal cannot be reconstructed using the quintic polynomial, but it has to be estimated in another way.

It is worth noting that, while the proposed approach, based on a synthesized polynomial signal, may appear arbitrary, its effectiveness is proven by the final results shown in Section 5.

3.3.2. Estimation of the synthesized pressure signal

Due to its highly nonlinear behavior, the synthesized pressure signal P_s is estimated by using a nonlinear autoregressive exogenous (−input) model (NARX). A NARX is a recurrent dynamic network with feedback connections, which is often implemented to model the evolution of a system over time [30]. It can learn to predict a time series given past values of the same series; hence it is usually exploited to model nonlinear dynamic systems.

The general equation for the NARX model is:

$$y(t) = f\big(y(t-1), y(t-2), .., y(t-n_y), \mathbf{x}(t), \mathbf{x}(t-1), .., \mathbf{x}(t-n_u)\big) \tag{6}$$

where y(t) *is* the next value of the dependent output signal which is regressed on n_y previous values of the output signal and n_u previous values of an independent input signal **x**(t). The function *f* represents the approximation of the physical relationship between the input and the output that the NARX tries to estimate. In our case the network is supposed to reconstruct the $P_s(t)$ pressure signal knowing the current and the future pressure measurements ($P_m(t)$ and $P_m(t+1)$), the actual time from the start of the braking and the reconstructed pressure signal of 3 time steps before (namely $P_s(t\text{-}3)$, $P_s(t\text{-}2)$ and $P_s(t\text{-}1)$). So the Eq. (1) can be rewritten as:

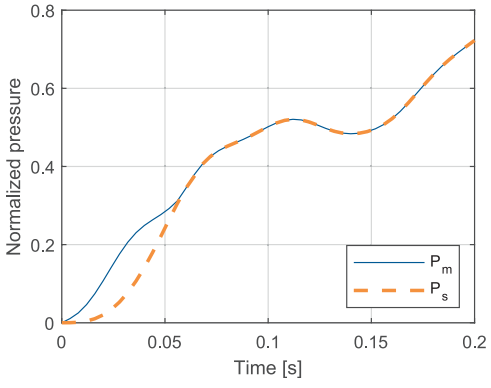

Fig. 4. Normalized pressure in the build-up phase, comparison between measured signal (P_m) and synthesized signal (P_s).

$$y(t) = f(y(t-1), y(t-2), y(t-3), \mathbf{x}(t)) \tag{7}$$

where

$$\mathbf{x}(t) = \begin{Bmatrix} P_m(t) \\ P_m(t+1) \\ t \end{Bmatrix} \tag{8}$$

$$y(t) = P_{NARX}(t) \tag{9}$$

where P_{NARX} indicates the estimate for the pressure signal P_s, which, as explained in Section 3.3.1, can not be synthesized in case the braking torque can not be measured directly. Note that the future value of the measured pressure signal ($P_m(t+1)$) is available because this procedure is performed on a dataset previously recorded (i.e. not in real time). Fig. 5 represents a diagram of the so called closed-loop arrangement of the network. This configuration is used to perform an iterated prediction of the modified pressure signal through multiple time steps. The NARX model is implemented using a two-layer feedforward neural network for the approximation of the function f.

As the diagram shows there is not much difference with respect to a conventional ANN except from the fact that at every iteration, the output is loaded on the feedback delayed line and it is used in the next one for the calculation of the following sample. During training the algorithm use the data available and the relative labels to optimize and adapt some internal parameters (weight matrices $\mathbf{IW}_{1,1}$, $\mathbf{LW}_{1,3}$, $\mathbf{LW}_{2,1}$ and the bias arrays $\mathbf{b}_1$, $\mathbf{b}_2$) so that it performs well on future unseen data. In addition to the usual weigth matrix associated to the input $\mathbf{IW}_{1,1}$ and its bias array $\mathbf{b}_1$, the NARX architecture is provided with another set of parameters stored in the $\mathbf{LW}_{1,3}$ matrix that multiplies directly the array composed of the previous 3 outputs of the time series. This array is stored and fed back through the feedback delayed line. The latter updates every time step removing the first element that entered in the array and storing the latest output computed by the network. As it happens for standard ANN, f_1 and f_2 are the activation functions of each layer.

During training, since the true outputs are available, the network architecture is switched to an open-loop configuration, so that the true outputs are used instead of feeding back the estimated ones, as shown in Fig. 6.

This has two advantages: the first is that the input to the feedforward network is more accurate. The second is that the resulting network has a purely feed-forward architecture, and the conventional backpropagation can be used for updating the internal parameters of the network. All of the training is done in open loop including the validation and testing steps. The typical workflow starts with the creation of the network in open loop, and only when it has been trained it is transformed to closed loop for multistep-ahead prediction.

3.3.3. *Pressure signal and experimental friction coefficient correction*

The results obtained with the trained NARX network are reported in Fig. 7a. The synthesized pressure signal is accurately reconstructed during the initial part of the braking maneuver.

Since significant discrepancies between the trends of the measured pressure and torque signals are observed only during the pressure build-up phase, the original pressure signal, P_m, can be used in the subsequent phases. To this purpose, a MATLAB function that takes as input the measured pressure P_m and outputs a "corrected" pressure signal, referred to as P_c, is implemented. In particular, the function uses the estimated signal P_{NARX} for the initial part of the braking and then smoothly passes to the pressure measurement P_m, when the two are no longer different (Fig. 7b). Taking k as the increasing counter that identifies the samples related to the discrete time history of a specific braking maneuver (with k restarting from 1 for each maneuver), the k_ε-*th* sample is the first sample of the maneuver for which the following condition is satisfied:

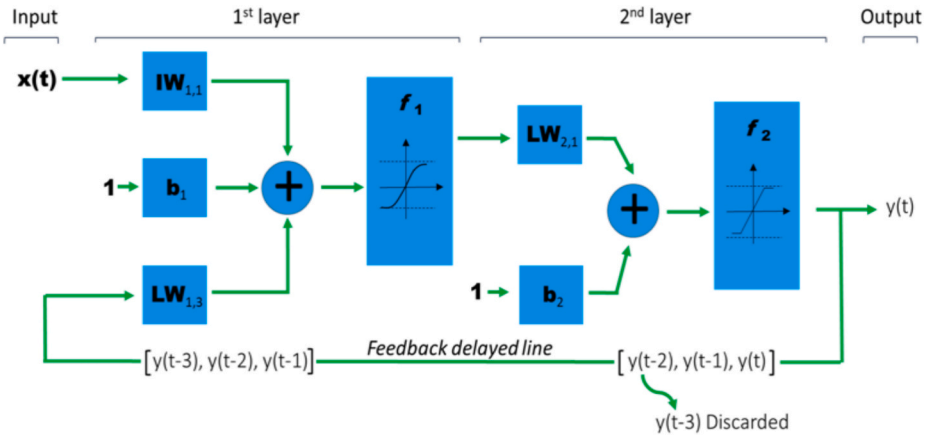

Fig. 5. NARX network closed loop architecture.

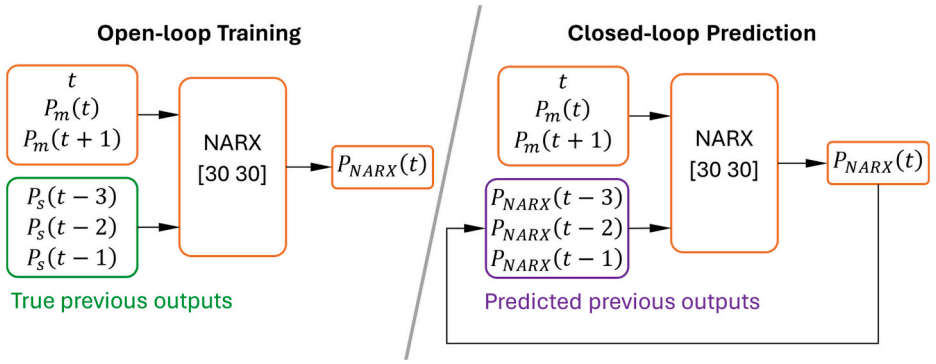

Fig. 6. NARX network open loop vs closed loop architecture comparison.

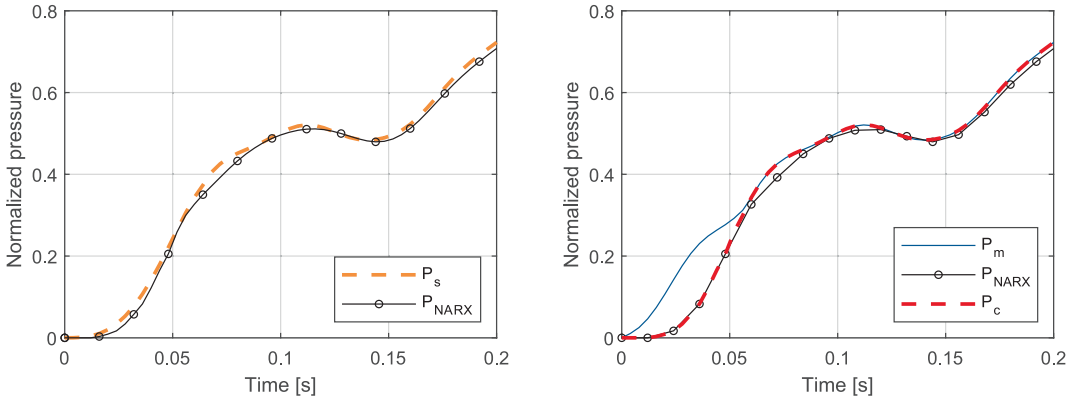

Fig. 7. Results of the NARX network, (a) synthesized pressure estimate (P_{NARX}) and (b) corrected pressure signal (P_c) generated by the merging function.

$$k_\varepsilon \neq 1 \wedge |P_{NARX}(k_\varepsilon) - P_m(k_\varepsilon)| \leq \varepsilon_P \tag{10}$$

with ε_p being an arbitrarily threshold. Hence, the signal P_c generated by the merging function is given by the following analytical expression:

$$P_c(k) = \begin{cases} P_{NARX}(k) & k < k_\varepsilon \\ P_m(k) & k \geq k_\varepsilon \end{cases} \tag{11}$$

Using the "corrected" pressure P_c allows to calculate from Eq. (3) more realistic friction coefficient values for the ground truth signal μ_{exp}, to be adopted in the next steps of the study. The benefit of this approach can be appreciated in Fig. 8, which reports the graph of a full braking maneuver and the pressure build-up phase of the following one. The effects of the combined application of the pressure threshold P_{th} can be also appreciated, as the friction coefficient is forced to μ_{const} (i.e. to 1 in the normalized plot) at the end of the braking maneuvers.

4. ML-based algorithm for friction coefficient estimation and torque calculation

As already anticipated in the Introduction, the research is aimed at implementing a robust method for calculating the braking torque on the front wheel of the motorcycle, in order to improve the prediction of the physical model obtained with a constant friction coefficient.

To this purpose, a ML algorithm capable of identifying the friction coefficient of the brake in any operating condition is developed using the MATLAB® software package (MathWorks, Natick, MA, USA). This section describes all the steps taken to design the proposed tool.

4.1. ANN implementation for friction coefficient estimation

Based on preliminary results (not reported in this paper), ANNs had been identified as very promising tools among supervised learning algorithms, and have been therefore investigated. Many different combinations of hyperparameters (e.g. hidden layers,

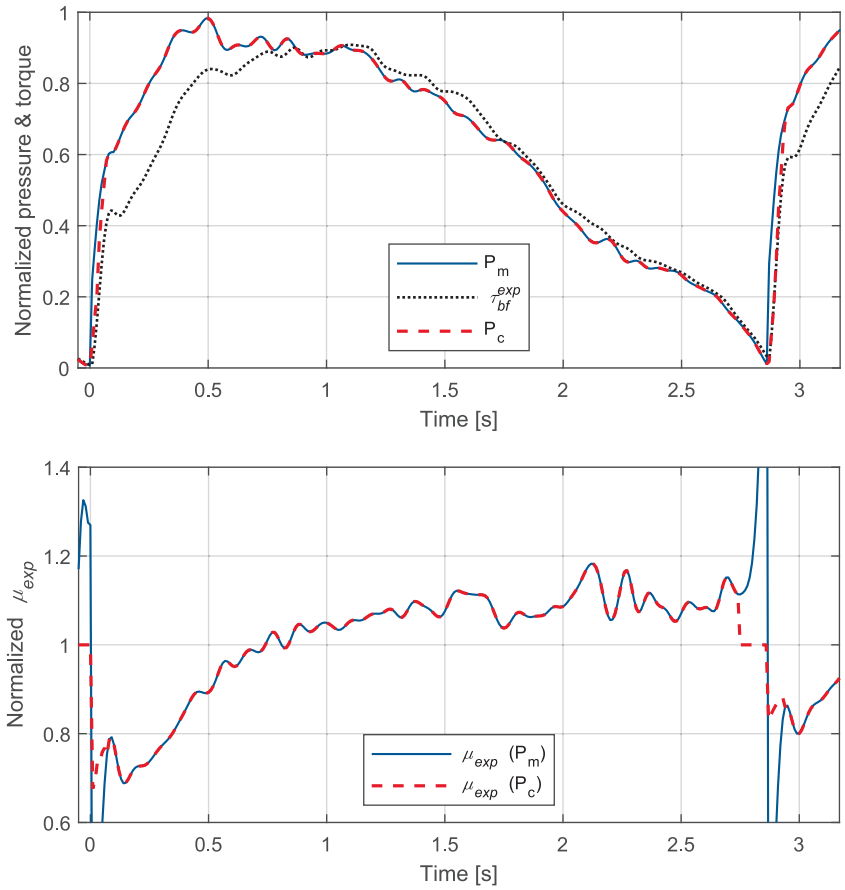

Fig. 8. (a) Normalized torque and pressure signals for the calculation of the true friction coefficient; (b) computed friction coefficient (normalized).

neurons per hidden layer, activation functions, training epochs, etc.) have been tested, to find the most suitable architecture for the regression problem of interest. In particular, a number of hidden layers ranging from 1 to 3 has been evaluated; moreover, a number of neurons ranging from 5 to 45 for each hidden layer has been evaluated.

The general architecture of the ANN considered for the first assessment is shown in Fig. 9. The layers were fully connected. Initially, only three inputs were taken into account, namely T_{acp}, P_c and ω_r, which are expected to constitute the most relevant variables affecting the friction coefficient. In particular, the input vector fed to the network contains the measurements related to a specific time step. The estimated instantaneous friction coefficient μ was the only output.

The different networks were trained by using the dataset acquired on racetrack A, namely the one where most of the tests are conducted. In order to speed up the process, a restricted portion of such dataset, referred to as TR-A1 was selected. The restricted

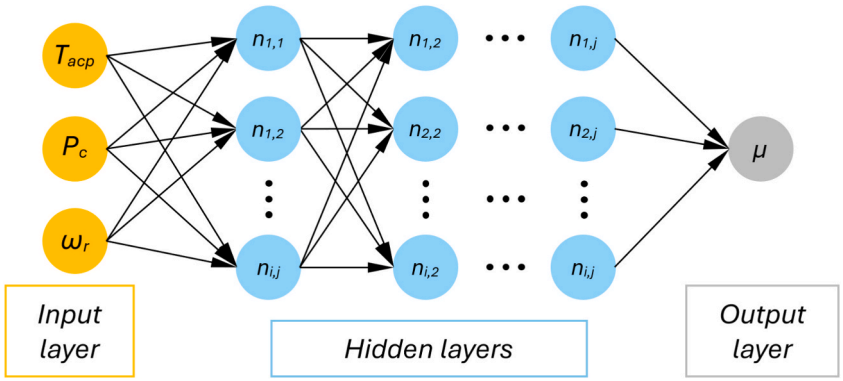

Fig. 9. General starting architecture of the ANN.

dataset TR-A1 was divided into training (60 %), validation (20 %) and testing (20 %) sets. The data belonging to each set were selected randomly, i.e. input vectors related to the same braking maneuver may be included in any of the three sets. Consistently with the considerations expressed in Section 3.3.3, input vectors containing a value of the brake fluid pressure P_c lower than the established threshold P_{th} are deemed unreliable and not fed to the network. In this phase, the values of the input vector are also used to compute the ground truth for the friction coefficient at the corresponding time step through Eq. (3), which is fed to the network as well. Before training, all the inputs are normalized to the range $[-1; 1]$. Regularization was also adopted to limit possible overfitting issues.

The most promising results were obtained by using a network with the following main hyperparameters: 2 hidden layers, each one having 10 neurons; activation functions, hyperbolic tangent sigmoid transfer function for the hidden layers (*tansig*) and symmetric saturating linear transfer function (*satlins*) for the output layer; training over a maximum of 350 epochs; maximum validation checks equal to 10. For this architecture, no parameter is penalized by regularization. As expected, complex ANNs appeared more prone to overfitting.

To quantitatively assess the accuracy of the selected ANN (referred to as estimation method E1 hereafter), the root mean square error (RMSE) has been evaluated. Since the braking torque τ_{bf}^{exp} is the quantity directly measured in the experiments, the RMSE has been evaluated by comparing such value with the torque τ_{bf}^{mod} calculated from Eq. (2) by using the friction coefficient estimated by the ANN.

The performance of E1 in terms of accuracy (RMSE) and speed (computational time required to predict 10^5 output values) is shown in Table 2. The RMSE has been computed for the normalized braking torque over the training dataset TR-A1. For the sake of comparison, the RMSE that would be obtained by using only the constant friction coefficient μ_{const} over the same dataset (referred to as E0) is also reported. The ANN appears quite promising, as the RMSE is reduced by more than 50 %.

4.2. Evaluation of alternative ML algorithms

The possible use of alternative algorithms for estimating the friction coefficient has been investigated with the same inputs and the same dataset TR-A1 used in Section 4.1 for defining the ANN. The analysis focused on two supervised learning algorithms, namely Support Vector Machines (SVMs) and Decision Trees (DTs). By Using the *regression learner* tool in MATLAB, the following algorithm formulations have been tested, to optimize hyperparameters:

- E2: SVM with linear Kernel
- E3: SVM with cubic Kernel
- E4: medium DT
- E5: fine DT

In addition, a LightGBM framework (E6) was implemented with Python and then converted into a Matlab library (which is a requirement of the final algorithm) to be also tested.

Table 2 shows the best results obtained for all the tested algorithms. tested plus the neural network previously described. As expected, linear SVMs do not appear suitable for the problem of interest. Conversely, the SVM with cubic Kernel succeeds in improving the braking torque estimate with respect to E0, but it appears remarkably less accurate and slower than E1. As for the DTs, they exhibit an accuracy comparable to the ANN, and a remarkably higher prediction speed. Finally, the LightGBM seems the most accurate. Conversely, its speed does not appear satisfactory, but this performance may be hampered by a non-optimized dll.

Therefore, the ANN (E1), the fine DT (E5, as priority is given to the best accuracy) and the LightGBM (E6) have been further investigated for possibly enhancing their performance.

4.3. Tuning of the selected ML algorithms

4.3.1. Tuning of the algorithm E1

The ANN has been trained again over the complete dataset available for racetrack A, i.e. TR-A2. The set of features preliminarily tested, i.e. the input vector consisting in T_{acp}, P_c and ω_r, was expanded with additional signals available or calculated from the telemetry deemed possibly relevant to the braking performance. In particular, the following signals have been considered:

Table 2
Performance evaluation of different algorithms.

Algorithm		Performance	
Code	Type	RMSE	Computational time [s]
E0	μ_{const}	$3.22 \bullet 10^{-2}$	/
E1	ANN	$1.44 \bullet 10^{-2}$	0.0108
E2	SVM	$4.09 \bullet 10^{-2}$	0.1923
E3	SVM	$2.52 \bullet 10^{-2}$	0.2273
E4	DT	$1.24 \bullet 10^{-2}$	0.0036
E5	DT	$1.13 \bullet 10^{-2}$	0.0040
E6	LightGBM	$0.87 \bullet 10^{-2}$	0.0660

1. Initial disc temperature (T_i): step signal containing the temperature measured by the single spot infrared sensor mounted on board at the beginning of each braking maneuver, which is kept constant for the duration of the entire maneuver.
2. Dissipated energy (E_{diss}): estimate of the cumulative energy dissipated during a braking maneuver, obtained by integrating over time the instantaneous braking power, given by the product of τ_{bf}^{mod} (estimated using Eq. (2) with μ_{const}) and ω_r.
3. Tarmac temperature (T_{track}): constant signal measured by the racing team at the beginning of each test and included in the telemetry after a test session.
4. Braking time (t): sawtooth signal that keeps track of the time elapsed from the beginning of each braking maneuver (t is reset to zero when a new braking maneuver starts).
5. Braking maneuver duration (t_e): step signal containing the total time of each maneuver, kept constant for the duration of the whole maneuver (it is worth noting that such value can be known at each time step because the analysis is performed in post-processing, not in real time).
6. Single spot and 1D-FE model temperature difference (ΔT): signal obtained from the instantaneous difference between the temperature measured by the infrared sensor mounted on board and T_{acp}.

Then, an input pruning algorithm has been implemented to remove the least salient input nodes from the first layer [31]. T_i, t and ΔT were identified as the most relevant features among the additional inputs. Therefore E_{diss}, T_{track} and t_e were discarded in the updated algorithm. Moreover, the hyperparameters have been reassessed, except for the number of hidden layers, which was kept equal to 2. The dataset TR-A2 was divided into training (57.2 %), validation (23 %) and testing (19.8 %) sets. Unlike in the previous analysis, the data were not divided randomly, but all the samples related to a specific maneuver were included in the same set, to have a better control of the training procedure. This explains the unusual percentages adopted for partitioning the dataset.

After the new training, the hyperparameters of the optimal ANN were modified as follows: 6 total inputs, with T_i, t and ΔT added to the previous ones (i.e. T_{acp}, P_c and ω_r); maximum validation checks equal to 20. The other hyperparameters were not changed. In particular, 10 neurons in each of the two hidden layers were confirmed as the most convenient architecture.

The trained network has been tested on a dataset completely unseen in the training phase, namely TR-B, in order to verify its actual generalization capabilities. The results provided by the updated E1 algorithm are shown in Table 3. The results achieved with the approach E0 (constant friction coefficient) are also reported. In order to compare the accuracy of the two approaches, the variation of the RMSE (Δ_{RMSE}) has been calculated as well.

It can be observed that the tested dataset TR-B is labelled as being related to a track with average disc temperature (see Table 1). In such an instance, the constant friction approximation is still acceptable. Nonetheless, the algorithm E1 can improve the torque estimation by more than 22 %, which is deemed a remarkable accuracy enhancement for a racing application.

4.3.2. Tuning of the algorithm E5

Also the fine DT has been retrained with the dataset TR-A2, by using the expanded vector of 6 input features defined in Section 4.3.1. The best results were obtained with a DT having the following hyperparameters: depth equal to 7; number of leaves equal to 101.

Then the updated algorithm E5 has been tested on the dataset TR-B. The results provided by the optimal DT, in terms of RMSE and Δ_{RMSE} are reported in Table 3. The enhancement in the estimation accuracy appears almost halved with respect to method E1, reasonably due to overfitting.

In order to possibly solve the overfitting issue, the implementation of a Minimal Cost-Complexity Pruning approach (MCCP [24]) has been attempted. A new DT has been trained with the dataset TR-A2 and then MCCP has been applied, obtaining a DT featuring a depth of 9 and 56 leaves. The results provided by the pruned DT (labelled as E5 + MCCP) for the dataset TR-B have been included in Table 3 as well. It can be observed that the MCCP algorithms succeeds in significantly improve the accuracy. Nonetheless, the performance of the DT appears still inferior to the one provided by the ANN. Therefore, the latter ML algorithm (E1) has been preferred for implementation in the data processing package used by the racing team.

4.3.3. Tuning of the algorithm E6

Similarly to the algorithms E1 and E5, the algorithm E6 has been retrained by using the dataset TR-A2, with the expanded vector of 6 input features. The best performance was achieved with the following hyperparameters: maximum number of leaves in one tree equal to 200; minimal number of data in one leaf equal to 7.

Table 3 shows the performance of the updated E6 algorithm tested on the dataset TR-B. The accuracy appears slightly superior to the E1 algorithm, hence E6 being promising. Nonetheless, the algorithm E1 has been preferred for implementing the final estimation

Table 3
Performance evaluation of the updated algorithms with respect to the E0 approach.

Algorithm	TR-B	
	RMSE	Δ_{RMSE} *[%]*
E0	$5.88 \bullet 10^{-2}$	/
E1	$4.55 \bullet 10^{-2}$	−22.6
E5	$5.20 \bullet 10^{-2}$	−11.5
E5 + MCCP	$4.87 \bullet 10^{-2}$	−17.1
E6	$4.40 \bullet 10^{-2}$	−25.2

tool, also in light of the results of further tests reported in Section 5.1.

4.4. Final architecture of the algorithm

The final architecture of the algorithm for estimating the braking torque with the sensor setup available in racing configuration is shown in Fig. 10. At each time step, t, of a braking maneuver, the following operations are performed to determine the instantaneous value of τ_{bf}^{mod}.

- The measured brake fluid pressure, P_m, is processed through the NARX algorithm and the subsequent merging function, to obtain the corrected pressure signal P_c.
- The disc temperature measured by the single spot sensor, T_d, is processed by a combination of 1D-FE thermal model and UKF state estimator, to predict the average temperature of the disc/pad contact patch, T_{acp}. The difference between T_d and T_{acp}, ΔT, is also computed, as additional input to the ANN.
- The computed signals T_{acp}, ΔT and P_c, together with the other signals directly extracted from the dataset (ω_r, t and Ti) are fed as inputs to the ANN.
- The instantaneous friction coefficient μ, estimated by the ANN, is used in combination with the corrected pressure P_c to update the brake model and estimate the instantaneous braking torque on the front wheel, τ_{bf}^{mod}.
- In case the value of P_c is below the defined threshold (P_{th}) and the considered time step is at the end of the braking maneuver (this condition is identified by half the duration of the maneuver, $t_e/2$), the ANN is bypassed: the braking torque is still computed by considering the corrected pressure P_c, but the constant friction coefficient μ_{const} is used instead.

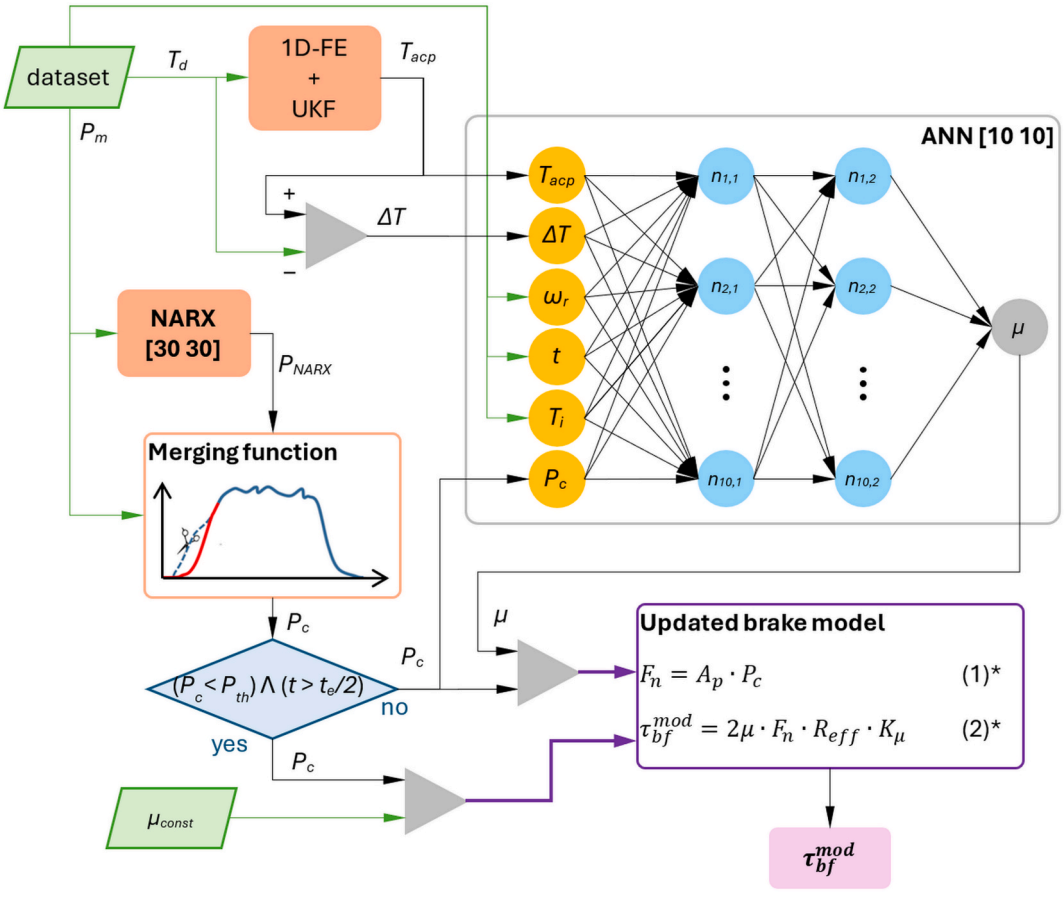

Fig. 10. Final architecture of the algorithm for braking torque estimation.

5. Results and discussion

5.1. Braking torque estimation

The performance of the whole algorithm E1, in terms of accuracy and computational time, has been assessed by processing 3 additional datasets not used during training, namely TR-M (average temperature), TR-H (high temperature) and TR-L (low temperature). High temperatures of the disc are typically experienced in racetracks where hard braking maneuvers are performed in close sequence, so that the discs have not enough time to cool down. Conversely, low temperatures are typically caused by rainy weather, that makes it difficult to keep the discs at an adequate temperature to operate properly.

Table 4 reports the RMSE value of each test and compares it with the performance achieved with μ_{const} (E0). The effectiveness of the algorithm E1 is confirmed in case of average temperatures (TR-M), the RMSE reduction keeping close to 23 %. An even better performance can be observed in case of high disc temperatures (TR-H), since the RMSE is reduced by more than one third. The accuracy improvement in case of low temperatures (TR-L) appears extremely high, as the reduction in the RMSE exceeds 60 %.

The algorithms E5 and E6, although not adopted for the final implementation of the torque estimation tool, have been tested with these three additional datasets as well, as a further check of their potential performance. The corresponding RMSE values and the comparisons with E0 are shown in Table 4. The accuracy of E5 does not appear sufficient. As for E6, a performance comparable with E1 has been achieved for average temperatures (TR-M) and low temperatures (TR-L). Conversely, in case of high disc temperatures (TR-H) the performance is poor. These results confirm the choice of E1 as the most convenient approach for the implementation of the final algorithm.

The measured and the estimated braking torque for two braking maneuvers are reported in Fig. 11, as examples to better understand how the algorithm E1 can improve the estimation accuracy. Fig. 11a is related to a hard-braking maneuver from dataset TR-H. As the disc temperature starts exceeding the range associated with the optimal performance (time of about 1 s), a fading-like effect is experienced, and the actual friction coefficient lowers and significantly diverge from the nominal value, causing the E0 approach to overestimate the torque considerably. The ANN can track the friction coefficient variation, hence permitting a more accurate braking torque estimation.

An apparently similar behavior can be observed in Fig. 11b, which shows a braking maneuver from dataset TR-L. In this case, the actual friction coefficient remains below the nominal value for the whole maneuver, because the low temperature makes the carbon disc to operate out of the optimal temperature range. This determines a significant overestimation of the braking torque when the E0 approach is adopted. Conversely, the torque estimated by the implemented algorithm E1 closely matches the measured one, thanks to an accurate estimation of the actual friction coefficient.

As for the computational time, the entire algorithm (including the estimation of the thermal behavior provided by the combination of 1D-FE model and UKF observer) could run stably in about 7.5 s/lap, hence meeting the desired specifications.

The results presented above confirm the effectiveness of the developed algorithm as a tool to accurately estimate the instantaneous friction coefficient and between the carbon disc and the pads and, in turn, the actual torque generated by the braking system, for a wide range of operating conditions that could be experienced during a race. The improvement on the previous constant-friction approach appears outstanding. The performance analysis also indirectly confirmed the suitability of the approach adopted to correct the measured pressure signal.

5.2. Friction coefficient map

In light of the successful assessment of the estimation performance, the developed algorithm has been used for processing also the datasets obtained from the telemetry in regular races (in which no torque measurements are available), to build a map of the friction coefficient covering the widest possible range of operating conditions.

The colormap shown in Fig. 12 reports the estimated friction coefficient as a function of the normalized braking power (horizontal axis) and of the normalized average temperature T_{acp} (vertical axis). The friction coefficient has been also normalized, by taking μ_{const} as the reference value: consequently, values higher than 1 (red tones) identify a friction coefficient greater than μ_{const}, while the opposite holds for blue tones; black areas mean that no data were available for the corresponding combination of operating conditions.

The friction coefficient map shows a wide region (colored in green\yellow) in which μ remains almost constant and close to its nominal value. This area represents the most recurring conditions that the brakes typically face in a race. Nonetheless, a strong dependency on both the temperature and the braking power can be also observed. The value of μ appears extremely sensible to low

Table 4
Performance comparison between the evaluated ML methods and constant friction coefficient approach.

Algorithm	Dataset					
	TR-M		TR-H		TR-L	
	RMSE	Δ_{RMSE} *[%]*	*RMSE*	Δ_{RMSE} *[%]*	*RMSE*	Δ_{RMSE} *[%]*
E0	$5.57 \bullet 10^{-2}$	/	$8.09 \bullet 10^{-2}$	/	$1.05 \bullet 10^{-1}$	/
E1	$4.27 \bullet 10^{-2}$	–23.2	$5.35 \bullet 10^{-2}$	–33.8	$4.09 \bullet 10^{-2}$	−61.1
E5	$4.88 \bullet 10^{-2}$	−12.3	$5.99 \bullet 10^{-2}$	−25.9	$6.06 \bullet 10^{-2}$	−42.3
E6	$4.13 \bullet 10^{-2}$	−25.8	$7.51 \bullet 10^{-2}$	−7.2	$4.11 \bullet 10^{-2}$	−60.9

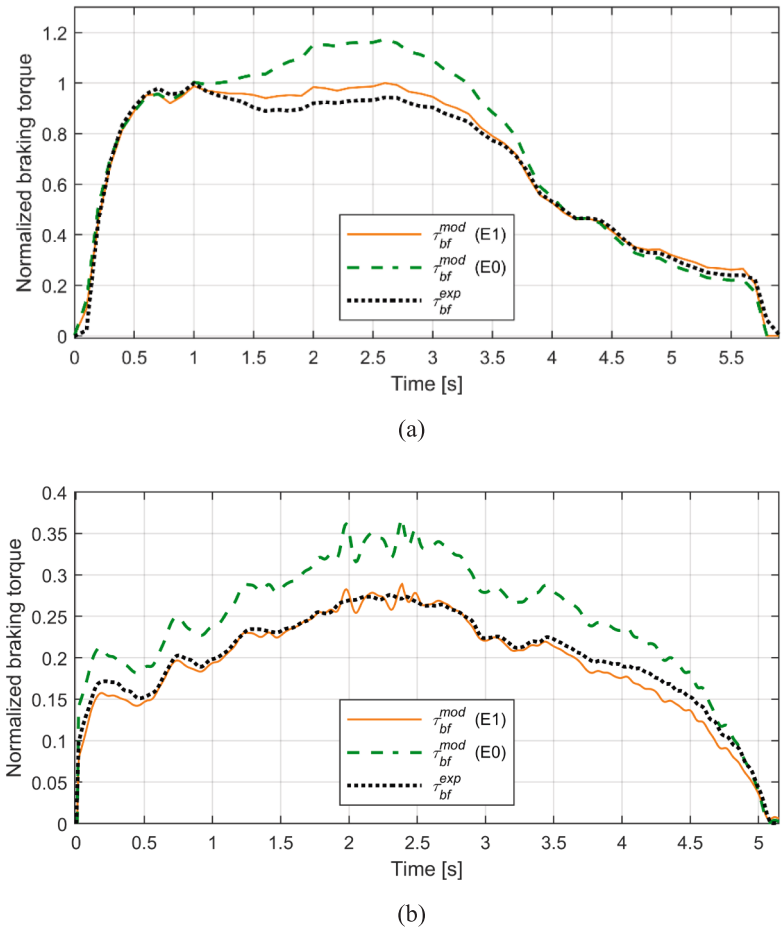

Fig. 11. Torque estimation, comparison between ANN (E1) and constant friction coefficient (E0) approach for a single braking maneuver from the dataset TR-H (a) and TR-L (b).

temperatures: as soon as the disc normalized temperature decreases under 0.3, the friction coefficient lowers of 20 % regardless of the braking power, hence causing the braking performance to drop considerably. On the other hand, beyond a normalized temperature of 0.55, the value of μ appears highly dependent on the braking power. A high braking power induces the fading phenomenon (visible on the upper right corner of the map). As a braking event for which fading has occurred progresses, the energy input into the friction interface lowers and the recovery phenomenon starts. Recovery may be gradual at first, can set in very aggressively towards the end of the stop, as shown in the upper left corner of the map.

The obtained map represents an extremely valuable outcome of the study. Indeed, it can be exploited to improve the prediction of the motorcycle performance in future events obtained through lap-time simulations, by refining the braking torque estimation for the all the operating conditions experienced over an entire lap of a racetrack.

6. Conclusions

This research activity focused on the estimation of the braking performance of MotoGP^{TM} class motorcycles equipped with carbon–carbon braking systems. In particular, it aimed at improving the accuracy of the braking torque estimate through machine learning techniques for identifying the actual friction coefficient value, hence permitting to overcome the limitations of the model currently used, which assumes a constant friction parameter.

A novel algorithm that combines a NARX and an ANN was developed, and its effectiveness was assessed by using a large dataset of measurements performed in racetrack tests:

- the implementation of the NARX brought about a big improvement in the dataset processing, since it could enhance the accuracy of the brake fluid pressure measurements through the definition of a corrected pressure signal;

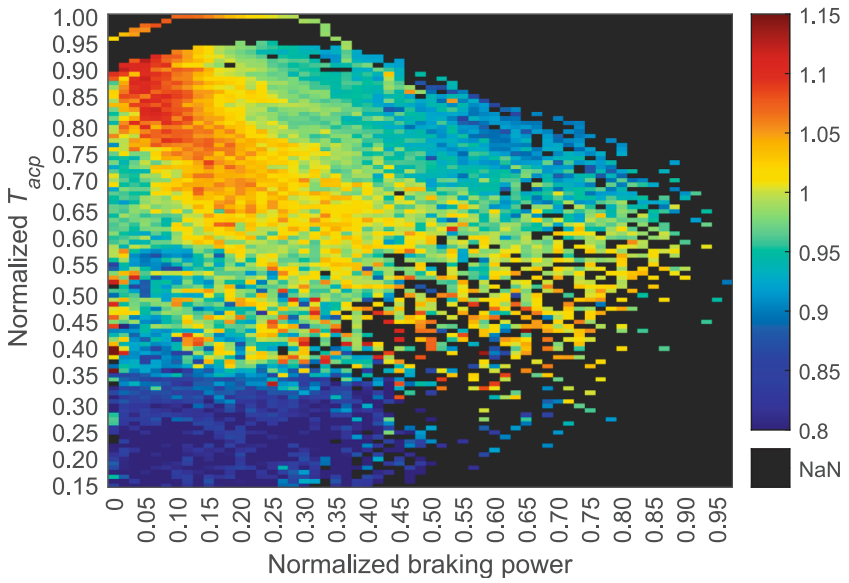

Fig. 12. Map of the friction coefficient estimated for different operating conditions.

- the ANN permitted to achieve an accurate estimate of the instantaneous friction coefficient characterizing the disc/pads contact region.

The developed algorithm was proven effective in predicting the braking torque with satisfactory accuracy, outperforming the constant friction coefficient approach for all the operating conditions of the disc.

Furthermore, it allowed to map the trend of the friction coefficient with respect to the main operating parameters of the braking system, namely disc average temperature and braking power, for most of the working conditions possibly encountered during a race. These results represent an essential tool for better predicting the braking performance in different scenarios, through numerical simulations. By simulating future events it is possible to tune in advance the braking system setup, hence possibly permitting to achieve better qualification and race results.

Finally, it is worth noting that the proposed approach has been already included in the data analysis package that is routinely used to process telemetry data by the company collaborating to the research.

CRediT authorship contribution statement

Federico Bonini: Conceptualization, Formal analysis, Investigation, Methodology, Software, Validation, Visualization, Writing – original draft. **Alessandro Rivola:** Funding acquisition, Supervision, Writing – review & editing. **Marco Troncossi:** Supervision, Writing – review & editing. **Alberto Martini:** Conceptualization, Formal analysis, Funding acquisition, Project administration, Supervision, Visualization, Writing – original draft, Writing – review & editing.

Declaration of competing interest

The authors declare that they have no known competing financial interests or personal relationships that could have appeared to influence the work reported in this paper.

Acknowledgments

Ducati Corse is kindly acknowledged for providing real data to test the developed methods. The Authors wish to thank particularly Dr. Nicolò Mancinelli for active collaboration and support.

Data availability

The data that has been used is confidential.

References

[1] G. Savage, Carbon-Carbon Composites, Springer Dordrecht, 1993, 10.1007/978-94-011-1586-5.

[2] W. Krenkel, B. Heidenreich, R. Renz, C/C-SiC composites for advanced friction systems, Adv. Eng. Mater. 4 (7) (2002) 427–436, https://doi.org/10.1002/1527-2648(20020717)4:7<427::AID-ADEM427>3.0.CO;2-C.
[3] C. Zhang, L. Zhang, Q. Zeng, S. Fan, L. Cheng, Simulated three-dimensional transient temperature field during aircraft braking for C/SiC composite brake disc, Mater. Des. 32 (5) (2011) 2590–2595, https://doi.org/10.1016/j.matdes.2011.01.041.
[4] J. Gururaja Rao, K.H. Sinnur, R.K. Jain, Effect of weave texture of carbon fabric on mechanical, thermal and tribological properties of carbon/carbon aircraft brakes, Int. J. Comp. Mater. 5 (5) (2015) 89–96, https://doi.org/10.5923/j.cmaterials.20150505.01.
[5] D. Junjie, Z. Menghang, C. Pengju, L. Zhuan, P. Liang, X. Peng, L. Yang, Tribological behavior and applications of carbon fiber reinforced ceramic composites as high-performance frictional materials, Ceram. Int. 47 (14) (2021) 19271–19281, https://doi.org/10.1016/j.ceramint.2021.02.187.
[6] Z. Stadler, K. Krnel, T. Kosmač, Friction and wear of sintered metallic brake linings on a C/C-SiC composite brake disc, Wear 265 (3–4) (2008) 278–285, https://doi.org/10.1016/j.wear.2007.10.015.
[7] M. Hao, R. Luo, Z. Hou, W. Yang, Q. Xiang, C. Yang, Effect of fiber-types on the braking performances of carbon/carbon composites, Wear 319 (2014) 145–149, https://doi.org/10.1016/j.wear.2014.07.023.
[8] S. Fan, L. Zhang, L. Cheng, G. Tian, S. Yang, Effect of braking pressure and braking speed on the tribological properties of C/SiC aircraft brake materials, Compos. Sci. Technol. 70 (2010) 959–965, https://doi.org/10.1016/j.compscitech.2010.02.012.
[9] A.A. Yevtushenko, P. Grzes, A. Adamowicz, The temperature mode of the carbon-carbon multi-disc brake in the view of the interrelations of its operating characteristics, Materials 13 (8) (2020) 1878, https://doi.org/10.3390/ma13081878.
[10] V. Ricciardi, D. Savitski, K. Augsburg, V. Ivanov, Estimation of brake friction coefficient for blending function of base braking control, SAE Int. J. Passeng. Cars - Mech. Syst. 10 (3) (2017) 774–785, https://doi.org/10.4271/2017-01-2520. Erratum published in SAE Int. J. Passeng. Cars - Mech. Syst. 12:3 (2019) 237-238. DOI: 10.4271/2017-01-2520.1.
[11] V. Ricciardi, K. Augsburg, S. Gramstat, V. Schreiber, V. Ivanov, Survey on modelling and techniques for friction estimation in automotive brakes, Appl. Sci. 7 (9) (2017) 873, https://doi.org/10.3390/app7090873.
[12] G.P. Ostermeyer, On the dynamics of the friction coefficient, Wear 254 (2003) 852–858, https://doi.org/10.1016/S0043-1648(03)00235-7.
[13] M. Marian, S. Tremmel, Current trends and applications of machine learning in tribology—a review, Lubricants 9 (9) (2021) 86, https://doi.org/10.3390/lubricants9090086.
[14] V. Ćirović, D. Aleksendrić, Development of neural network model of disc brake operation, FME Transactions 38 (2010) 29–38.
[15] D. Aleksendrić, D.C. Barton, Neural network prediction of disc brake performance, Tribol. Int. 42 (2009) 1074–1080, https://doi.org/10.1016/j.triboint.2009.03.005.
[16] D. Aleksendrić, Č. Duboka, Prediction of automotive friction material characteristics using artificial neural networks-cold performance, Wear 261 (2006) 269–282, https://doi.org/10.1016/j.wear.2005.10.006.
[17] I. Mutlu, Artificial neural networks modelling of non-asbestos brake lining performance boric acid in brake pad, Inform. Technol. J. 8 (3) (2009) 398–402, https://doi.org/10.3923/itj.2009.398.402.
[18] A. Senatore, V. D'Agostino, R. Di Giuda, V. Petrone, Experimental investigation and neural network prediction of brakes and clutch material frictional behaviour considering the sliding acceleration influence, Tribol. Int. 44 (10) (2011) 1199–1207, https://doi.org/10.1016/j.triboint.2011.05.022.
[19] V. Ćirović, D. Aleksendrić, Dynamic modeling of disc brake contact phenomena, FME Trans. 39 (2011) 177–183.
[20] G. Xiao, Z. Zhu, Friction materials development by using DOE/RSM and artificial neural network, Tribol. Int. 43 (1–2) (2010) 218–227, https://doi.org/10.1016/j.triboint.2009.05.019.
[21] M.P. Deisenroth, A.A. Faisal, C.S. Ong, Mathematics for Machine Learning, Cambridge University Press, 2020.
[22] I. Goodfellow, Y. Bengio, A. Courville, Deep Learning, MIT Press, 2016.
[23] C. Cortes, V. Vapnik, Support-vector networks, Mach. Learn. 20 (3) (1995) 273–297.
[24] L. Breiman, J. Friedman, C.J. Stone, R.A. Olshen, Classification and Regression Trees, CRC Press, 1984, 10.1201/9781315139470.
[25] G. Ke, Q. Meng, T. Finley, T. Wang, W. Chen, W. Ma, Q. Ye, T.-Y. Liu, LightGBM: a highly efficient gradient boosting decision tree, in: Proceedings of the 31st International Conference on Neural Information Processing Systems (NIPS'17), Curran Associates Inc., Red Hook, NY, USA, 2017, pp. 3149–3157.
[26] S. Sarkka, Bayesian Filtering and Smoothing, Cambridge University Press, 2013.
[27] M.C. Best, A.P. Newton, S. Tuplin, The identifying extended Kalman filter: parametric system identification of a vehicle handling model, Proc. Inst. Mech. Eng., Part K: J. Multi-Body Dyn. 221 (1) (2007) 87–98, https://doi.org/10.1243/14644193JMBD68.
[28] S. Julier, J. Uhlmann, H.F. Durrant-Whyte, A new method for the nonlinear transformation of means and covariances in filters and estimators, IEEE Trans. Autom. Control 45 (3) (2000) 477–482, https://doi.org/10.1109/9.847726.
[29] F. Bonini, A. Rivola, A. Martini, Novel unscented Kalman filter-based method to assess the thermal behavior of carbon brake discs for high-performance motorcycles, Int. J. Thermofluids 21 (2024) 100547, https://doi.org/10.1016/j.ijft.2023.100547.
[30] H. Xie, H. Tang, Y.H. Liao, Time series prediction based on NARX neural networks: an advanced approach, in: Proceedings of the 2009 International Conference on Machine Learning and Cybernetics, 2009, pp. 1275–1279, https://doi.org/10.1109/ICMLC.2009.5212326.
[31] A. Jain, D. Zongker, Feature selection: evaluation, application, and small sample performance, IEEE Trans. Pattern Anal. Mach. Intell. 19 (2) (1997) 153–158.